A novel function of sphingosine-1-phosphate to activate a non-selective cation channel in human endothelial cells

Katsuhiko Muraki and Yuji Imaizumi

Department of Molecular and Cellular Pharmacology, Graduate School of Pharmaceutical Sciences, Nagoya City University, Mizuhoku, Nagoya 467-8603, Japan

(Resubmitted 2 July 2001; accepted 8 August 2001)

1. The Ca^{2+} entry pathway activated by sphingosine-1-phosphate (S1P) was examined in primary cultured vascular endothelial cells dispersed from human umbilical vein (HUVECs) by measuring intracellular Ca^{2+} concentration ($[Ca^{2+}]_i$), whole-cell membrane currents and single channel activity.

2. Application of S1P to HUVECs induced a slowly developing, sustained increase in $[Ca^{2+}]_i$. When Ca^{2+} was absent from the bathing solution, no S1P-induced changes in $[Ca^{2+}]_i$ were observed. Tert-butylhydroquinone (BHQ), an inhibitor of Ca^{2+} pumps in endoplasmic reticulum, and histamine induced a transient elevation of $[Ca^{2+}]_i$ in HUVECs.

3. Pretreatment of HUVECs with 100 ng ml^{-1} pertussis toxin (PTX) for 15 h almost abolished the S1P effect on $[Ca^{2+}]_i$ and reduced the histamine effect to 40 % of the control. The BHQ-induced elevation of $[Ca^{2+}]_i$ was insensitive to PTX.

4. When whole-cell membrane currents were recorded using the amphotericin B-perforated-patch clamp technique while monitoring $[Ca^{2+}]_i$, application of S1P induced a tiny inward current (I_{S1P}) which was followed by the elevation of $[Ca^{2+}]_i$. I_{S1P} reversed at $+20.0 \pm 2.7$ mV under these experimental conditions.

5. When S1P was included in the pipette solution in the excised inside-out patch clamp configuration, single channel activity with a conductance of 17 pS was activated. This channel activity depended on the presence of intracellular GTP.

6. In summary, these results show that S1P has a novel effect in mammalian cardiovascular endothelium to activate a non-selective cation (NSC) channel in a GTP-dependent manner via a PTX-sensitive G-protein. This S1P-sensitive NSC channel acts as a Ca^{2+} entry pathway in endothelium.

Treatment of human umbilical vein endothelial cells (HUVECs) with phorbol 12-myristate 13-acetate induces a novel gene, *edg-1* (endothelial differentiation gene-1), which encodes a GTP-binding protein (G-protein)-coupled receptor (GPCR) (Hla & Maciag, 1990). Several other GPCRs that have similar sequences to *edg-1*, such as *edg-2* to *edg-8* (*edgs*), have been isolated (Okazaki *et al.* 1993; Hecht *et al.* 1996; Yamaguchi *et al.* 1996; An *et al.* 1998; Pyne & Pyne, 2000). Edg-1, -3, -5, -6 and -8 are high affinity receptors for sphingosine-1-phosphate (S1P), a platelet-derived bioactive lipid (Yatomi *et al.* 1997; Lee *et al.* 1998; Wang *et al.* 1999; Pyne & Pyne, 2000). In many types of cell including vascular endothelial cells, stimulation of edg-1 with S1P is transduced by G-proteins, which are sensitive to pertussis toxin (PTX), and results in an elevation of intracellular Ca^{2+} concentration ($[Ca^{2+}]_i$), and/or activation of mitogen-activated protein (MAP) and Rho kinases (Lee *et al.* 1999; Ancellin & Hla, 1999). Recently, S1P has been shown to regulate angiogenesis and to stimulate wound healing. In endothelial cells, these effects require the activation of edg-1 and edg-3 (Lee *et al.* 1999; Wang *et al.* 1999; Lee *et al.* 2000). Recent studies have demonstrated that the development of the vasculature is stunted significantly in edg-1-deficient mice (Liu *et al.* 2000). Stimulation of edgs by S1P has also been shown to activate the endothelial isoform of nitric oxide synthase (Igarashi *et al.* 2001). S1P is also one of the key factors responsible for lipid-derived biological activities such as stress fibre and focal adhesion plaque formation, and cell migration (Hla *et al.* 1999). Thus the cellular and molecular mechanisms involved in the actions of S1P have been a focus of multidisciplinary investigations.

Although it has been reported that S1P elevates $[Ca^{2+}]_i$, the underlying mechanism is not understood fully. In particular, stimulation of edg-1, which couples to PTX-sensitive G-proteins and is independent of phosphoinositide turn-over, elevates $[Ca^{2+}]_i$ via an unknown

mechanism (Lee *et al.* 1999; Ancellin & Hla, 1999). Furthermore, it has been proposed that S1P directly releases Ca^{2+} from intracellular Ca^{2+} stores, i.e. S1P can act as an intracellular second messenger (Mattie *et al.* 1994; Van Brocklyn *et al.* 1998).

The main goal of the present study was to identify and characterize mechanisms involved in the elevation of $[Ca^{2+}]_i$ by S1P in human vascular endothelial cells. Our results identify a novel function of S1P as an activator of non-selective cation (NSC) channels in human endothelial cells. Preliminary results from this study have been reported in abstract form (Muraki & Imaizumi, 2001).

METHODS

Cell culture

Human umbilical vein endothelial cells (HUVECs) from umbilical cords obtained from full-term normal pregnancies (with ethical committee approval) were isolated by collagenase (0.2 mg ml^{-1}) digestion as previously described (Muraki *et al.* 1997). Cells were grown and maintained in Dulbecco's modified Eagle's medium (DMEM) supplemented with growth factors (Nisui, Tokyo, Japan), 10% fetal calf serum (FCS), penicillin G (100 units ml^{-1}) and streptomycin sulfate (100 mg ml^{-1}), at 37 °C under an atmosphere of 5% CO_2 and 95% room air. HUVECs were not used after the sixth passage. For electrophysiological experiments where single non-colonial cells were required, the cells were replated in DMEM (without growth factors and FCS) in 3.5 cm dishes coated with 0.2% gelatin (Wako, Tokyo, Japan). For measuring $[Ca^{2+}]_i$, growth factors and FCS were removed 48 h after replating. The purity of endothelial cell preparations was tested by indirect immunofluorescence staining using anti-von Willebrand factor (primary antibody, Dako, Denmark). All experiments were carried out at room temperature (25 ± 1 °C).

Measurement of $[Ca^{2+}]_i$

HUVECs were loaded with 2.5 μM fura-2 acetoxymethyl ester (fura-2 AM) in standard Hepes solution for 45 min at 37 °C. Measurement of fura-2 fluorescence signals was performed using the Argus 50/CA and Argus/HisCa imaging systems (Hamamatsu Photonics, Hamamatsu, Japan). The frequency of image acquisition was selected to be one image every ~1 and 10 s for simultaneous measurement of $[Ca^{2+}]_i$ and membrane currents, and for only $[Ca^{2+}]_i$ measurement, respectively. In some experiments, the ratios of fluorescence intensity were transformed into $[Ca^{2+}]_i$ using the following equation:

$$[Ca^{2+}]_i = 224B((R - R_{min})/(R_{max} - R)),$$

where R is the fluorescence ratio 340 nm/380 nm, R_{min} and R_{max} are the fluorescence ratio determined by addition of 1 mM EGTA and 2 mM Ca^{2+}, respectively, after the permeabilization of cells with 10 μM ionomycin, and B is the intensity of the fluorescence proportionality coefficients obtained at 380 nm under R_{min} and R_{max} conditions.

Electrophysiological recordings

Whole-cell membrane currents and membrane potentials were recorded with the amphotericin B-perforated-patch clamp technique using a List EPC7 amplifier (List, Germany). The resistance of microelectrodes filled with pipette solution was in the range 3–5 MΩ. Membrane currents and voltage signals were stored and analysed as described previously (Imaizumi *et al.* 1989; Taki *et al.* 1999). Briefly, membrane currents and voltage signals were monitored on a storage oscilloscope (VC-6041, Hitachi, Tokyo, Japan) and stored on videotape after being digitized by pulse code modulation (PCM) recording system (modified to acquire a DC signal, PCM 501ES; Sony, Tokyo, Japan). Data on tape were later downloaded onto a computer (IBM-AT compatible) using an analog–digital converter (Data Translation, DT2801A). Data acquisition and analysis for whole-cell and single channel currents were carried out using AQ/Cell-soft, developed in the laboratory of Dr Wayne Giles (University of Calgary), and single channel current analysis program V7.0C (PAT), developed by Dr John Dempster (University of Strathclyde). In some experiments, ramp waveforms were applied as a voltage clamp command using a multi-pulse generator (FS-1915; NF Electronics, Tokyo, Japan). All current records were filtered at 1 kHz (4-pole Bessel filter, NF Electronics). In some experiments, current signals were filtered at 300 Hz.

The relative open-state probability of channels (NP_o) was calculated using the following equation:

$$NP_o = \sum_{i=0}^{N} (it_i)/T,$$

where i is the number of channels open, t_i is the time spent with i channels open, N is the maximum number of open channels observed in the patch, P_o is the channel open probability and T is the sampling time. Since we did not define the total number of channels present in each patch membrane, we assumed the maximum number of unitary current levels observed in a patch to be equal to the number of active channels in the patch. The single channel data were sampled on the computer using the PAT software. Single channel events were detected using a half-amplitude criterion and the all-point amplitude histogram was fitted with the Gaussian distribution function. The permeability for K^+ (P_K), the only other permeable cation besides Na^+ in the intra- and extracellular solution, was measured relative to that of Na^+ (P_{Na}) from the reversal potential in the absence of extracellular Ca^{2+} (nominal Ca^{2+} free) using eqn (1):

$$P_K/P_{Na} = ([Na^+]_o - [Na^+]_i \exp(V_{rev}F/RT))/([K^+]_i \exp(V_{rev}F/RT) - [K^+]_o), \quad (1)$$

where V_{rev} is the reversal potential and F, R and T have their usual meanings. The permeability of Ca^{2+} relative to Na^+ was calculated from the reversal potential measured with 2.2 mM Ca^{2+} in the extracellular solution.

$$P_{Ca}/P_{Na} = (1 + \exp(V_{rev}F/RT)) \times (([Na^+]_i + \alpha[K^+]_i)\exp(V_{rev}F/RT) - [Na^+]_o - \alpha[K^+]_o)/4[Ca^{2+}]_o, \quad (2)$$

where α is P_K/P_{Na} obtained from eqn (1) using Ca^{2+}-free solution (Vennekens *et al.* 2000).

Solutions and drugs

The Ca^{2+}- and Mg^{2+}-free phosphate-buffered solution used for cell isolation contained (mM): NaCl 137, KCl 2.7, Na_2HPO_4 8.1 and KH_2PO_4 1.47. Standard Hepes (Dojindo, Kumamoto, Japan)-buffered solution of the following composition was used (mM): NaCl 137, KCl 5.9, $CaCl_2$ 2.2, $MgCl_2$ 1.2, glucose 14 and Hepes 10. The pH was adjusted to 7.4 with 10 N NaOH. Ca^{2+}-free Hepes-buffered solution was prepared by omitting Ca^{2+} from the standard Hepes solution (no EGTA). The (external) bathing solution for the excised inside-out patch clamp recording contained (mM): KCl 120, TEA-Cl 20, $MgCl_2$ 1 and Hepes 10. In some experiments, 120 mM KCl was replaced with equimolar CsCl. The pCa and pH of these solutions were adjusted to 7 and 7.4 using Ca^{2+}-EGTA buffer and 10 N KOH, respectively. The pipette solution for whole-cell recording contained (mM): potassium aspartate 110, KCl 30, $MgCl_2$ 4 and Hepes 10, with

amphotericin B (100–300 μg ml^{-1}). For the excised inside-out patch clamp recording, K^+ was replaced with Cs^+ and amphotericin B was omitted from the internal solution. The pH was adjusted to 7.2 with 10 N KOH. The following drugs were used: histamine (Wako, Osaka, Japan), sphingosine-1-phosphate (S1P, Cayman Chemical, Ann Arbor, USA), ionomycin (Sigma), PD98059 (Biomol, Plymouth, USA), tert-butylhydroquinone (BHQ, Wako), pertussis toxin (PTX, Sigma), sphingosine (SPH, Sigma), C6-ceramide (Cayman Chemical), SK&F96365 (Biomol) and wortmannin (Sigma). S1P was dissolved in 10 mM NaOH at 3 mM, divided into aliquots and stored at −80 °C. Before experiments, aliquots were diluted using the standard external solution with or without fatty acid-free bovine serum albumin (BSA). In most experiments, we did not use BSA to dissolve S1P since BSA itself sometimes induced a slight elevation of $[Ca^{2+}]_i$ in HUVECs. Both SPH and C6-ceramide were dissolved in dimethylsulfoxide (DMSO), and then diluted directly into the bathing solution to achieve the final concentration. Histamine was dissolved in distilled water to make 10 mM stock solution. All drugs except lipids and histamine were dissolved in DMSO (as 100 mM stock solutions). These solvents (distilled water and DMSO) had no effect on $[Ca^{2+}]_i$ or membrane currents, when the corresponding amount was applied by superfusion. Drug concentrations are expressed as the final concentration in the bathing solution. The pH of the solution was readjusted after the addition of drugs. Since lipids with a long carbon chain may have direct membrane effects, SPH, which has a similar structure to S1P, was used as a negative control compound.

Statistics

Data are expressed as means ± S.E.M. Statistical significance between two groups was examined using Student's t test. Statistical significance at P values of 0.05 and 0.01 is indicated in figures and text by * and **, respectively.

RESULTS

Effects of S1P on $[Ca^{2+}]_i$ in HUVECs

The effects of S1P on $[Ca^{2+}]_i$ in HUVECs are illustrated in Fig. 1. Here, we used histamine as a control substance to elevate $[Ca^{2+}]_i$ in HUVECs, because the characteristics of the histamine-induced effects are well known: they are mainly histamine H1 mediated and involve production of inositol trisphosphate ($InsP_3$) via activation of phospholipase C (PLC) (Hill *et al.* 1997). Application of 0.3 μM S1P significantly increased $[Ca^{2+}]_i$ (55.8 ± 4.0 and 236.5 ± 9.8 nM, $n = 10$, $P < 0.01$, Fig. 1*A*) and subsequent application of 3 μM histamine resulted in similar effects. Since lipid compounds with a long carbon chain may have direct membrane effects, HUVECs were exposed to SPH, which has a similar structure to S1P. In this negative control experiment, SPH (< 1 μM) had little effect on $[Ca^{2+}]_i$, although 3 μM SPH resulted in a slight elevation of $[Ca^{2+}]_i$ (from 73.8 ± 4.9 to 123.1 ± 23.7 nM, $n = 10$, Fig. 1*B* and *C*). C6-ceramide at 0.3 μM, another lipid which has a long carbon chain in the structure, also had no effect on $[Ca^{2+}]_i$ in HUVECs (not shown, $n = 15$). In contrast, addition of 0.3 μM S1P (a 10-fold lower concentration than that of SPH) effectively increased $[Ca^{2+}]_i$ to 214.3 ± 18.7 nM ($n = 10$). The rate of elevation of $[Ca^{2+}]_i$ after S1P application was much slower than that induced by histamine. After removal of S1P, $[Ca^{2+}]_i$ gradually decreased; nevertheless, washout for 10 min did not return $[Ca^{2+}]_i$ to the control level (Fig. 1*A* and *B*). In Fig. 1*C*, the Ca^{2+} responses of HUVECs to S1P and SPH are summarized as concentration–response relationships. The increases in $[Ca^{2+}]_i$ induced by S1P and SPH were normalized to that induced by 3 μM histamine and plotted against each concentration. The concentration of S1P required for a 50 % increase in $[Ca^{2+}]_i$ was estimated to be 63 nM. It is likely that S1P (< 1 μM) affects HUVECs without having non-specific membrane effects.

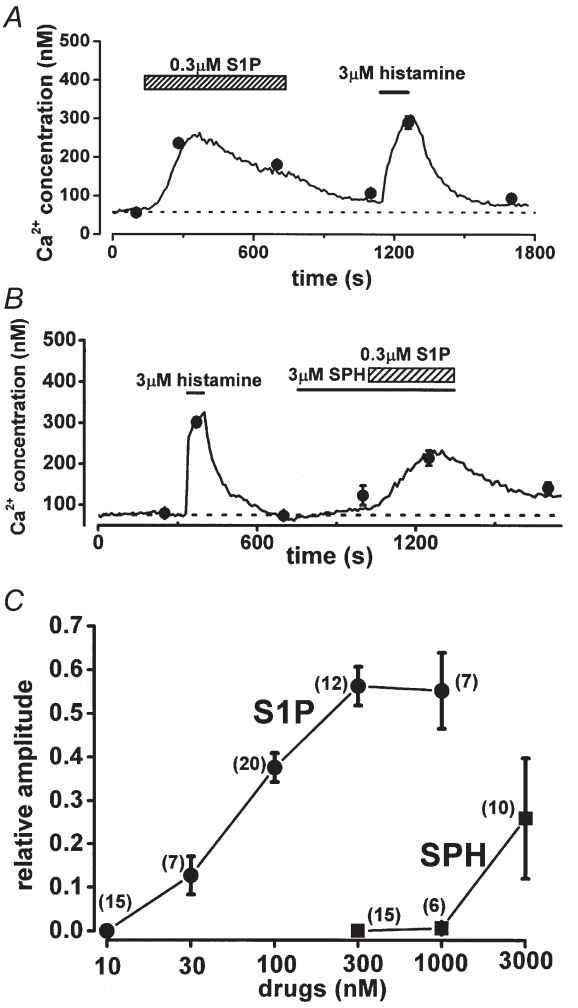

Figure 1. Elevation of $[Ca^{2+}]_i$ by S1P in HUVECs

A, serial application of 0.3 μM S1P and 3 μM histamine to HUVECs that were loaded with fura-2. *B*, effect of SPH on $[Ca^{2+}]_i$ in HUVECs and comparison with S1P-induced responses. The line shows the change in $[Ca^{2+}]_i$ obtained from a representative cell, and the averages (●) denote responses from 10 separate cells. *C*, summarized data describing the concentration–response relationship for the S1P and SPH effects. The increase in $[Ca^{2+}]_i$ induced by both compounds was normalized to that induced by 3 μM histamine and then plotted against concentration. Either S1P or SPH was applied once. Numbers in parentheses correspond to the number of cells studied.

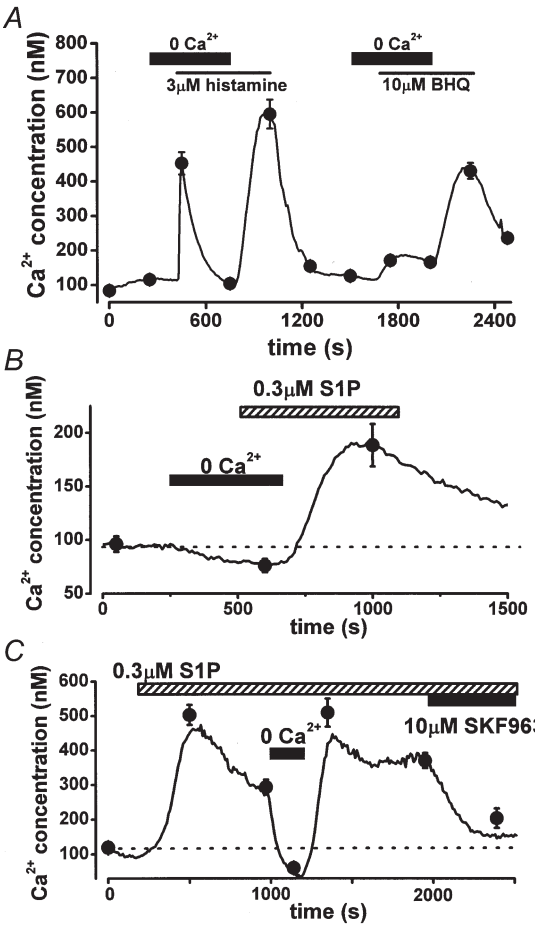

Figure 2. Ca^{2+} response to S1P, histamine and BHQ in the absence of external Ca^{2+} and the effect of SK&F96365 in HUVECs

After external Ca^{2+} was removed (0 Ca^{2+}, no EGTA), 3 μM histamine (*A*), 10 μM BHQ (*A*) or 0.3 μM S1P (*B*) was applied; subsequently 2.2 mM Ca^{2+} was added to the bathing solution in the presence of each agonist. *C*, in the presence of 0.3 μM S1P, external Ca^{2+} was removed for the duration indicated by the bar; subsequently, 10 μM SK&F96365 was applied. The line shows the change in $[Ca^{2+}]_i$ obtained from a representative cell. The averaged responses were from 10 separate cells.

Source of Ca^{2+} mobilized by S1P in HUVECs

To determine the source of the Ca^{2+} involved in the S1P-induced response, $[Ca^{2+}]_i$ in HUVECs was examined using a bathing solution lacking Ca^{2+}, and the response to S1P was compared with those to histamine and BHQ (Fig. 2). Even in the absence of external Ca^{2+}, application of 3 μM histamine or 10 μM BHQ induced a transient rise of $[Ca^{2+}]_i$, implying that these compounds activated Ca^{2+} release from Ca^{2+} stores (Fig. 2*A*). Addition of 2.2 mM Ca^{2+} in the presence of histamine and BHQ produced a large elevation of $[Ca^{2+}]_i$. In contrast, approximately 90% of HUVECs showed no response to 0.3 μM S1P in the absence of external Ca^{2+} (Fig. 2*B*). Following addition of Ca^{2+} to the bathing solution, S1P consistently elevated $[Ca^{2+}]_i$, suggesting that S1P actions are dependent upon external Ca^{2+} entry into the cell. The S1P-induced elevation lasted more than 5 min even after wash-out of S1P in most cells using a bathing solution containing 0.2% BSA. However,

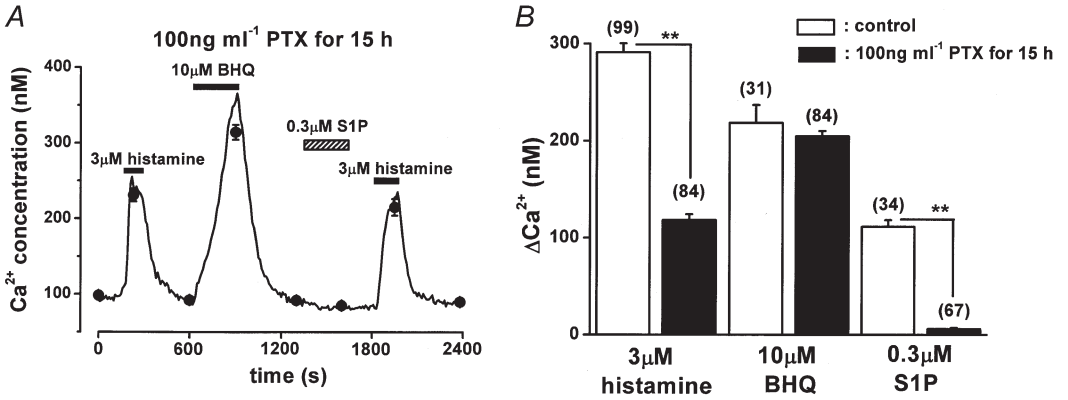

Figure 3. The effects of PTX on S1P-, histamine- and BHQ-induced Ca^{2+} responses in HUVECs

HUVECs were pretreated with 100 ng ml^{-1} PTX for 15 h. *A*, the line and filled circles show the change in $[Ca^{2+}]_i$ obtained from a representative cell and the averages from 10 separate cells, respectively. *B*, summary of the effects of PTX. Numbers in parentheses show the number of cells studied. ** $P < 0.01$.

10 % of HUVECs exhibited a transient elevation of $[Ca^{2+}]_i$ following S1P addition in the absence of external Ca^{2+}, although the elevation was much smaller than that by 3 μM histamine (13.3 $\pm$ 5.1 %, $n = 5$).

Figure 2*C* shows the effect of SK&F96365, an inhibitor of non-selective cation (NSC) channels, on the S1P-induced elevation of $[Ca^{2+}]_i$. SK&F96365 at 10 μM significantly inhibited the S1P-induced elevation of $[Ca^{2+}]_i$ (370.6 $\pm$ 22.0 and 203.6 $\pm$ 27.8 nM in the absence and presence of 10 μM SK&F96365, $n = 10$). This elevation of $[Ca^{2+}]_i$ was abolished by removal of external Ca^{2+}, and restored by the application of Ca^{2+}. These results indicate that activation of NSC channels and consequent Ca^{2+} entry from the extracellular space have an obligatory role in S1P-induced elevation of $[Ca^{2+}]_i$. In contrast, histamine and BHQ act via Ca^{2+} release from Ca^{2+} stores.

Signal transduction involved in Ca^{2+} response to S1P in HUVECs

The possible involvement of G-proteins in the S1P-induced Ca^{2+} response was examined using PTX. As shown in Fig. 3, after HUVECs were treated for 15 h with 100 ng ml^{-1} PTX, application of 3 μM histamine elevated $[Ca^{2+}]_i$ by 40.6 % of the control ($P < 0.01$ *vs.* control, Fig. 3*A* and *B*). In contrast, under the same experimental conditions, the change in $[Ca^{2+}]_i$ induced by 0.3 μM S1P was almost abolished (5.9 $\pm$ 1.1 nM, $n = 67$, $P < 0.01$ *vs.* control), while the BHQ-induced response was not affected by this treatment ($P > 0.05$ *vs.* control, Fig. 3*B*). The effects of wortmannin and PD98059, which are inhibitors of phosphatidylinositol 3 (PI3) kinase and MAP kinase, respectively, on the Ca^{2+} response to S1P were also examined. Neither pretreatment with 100 nM

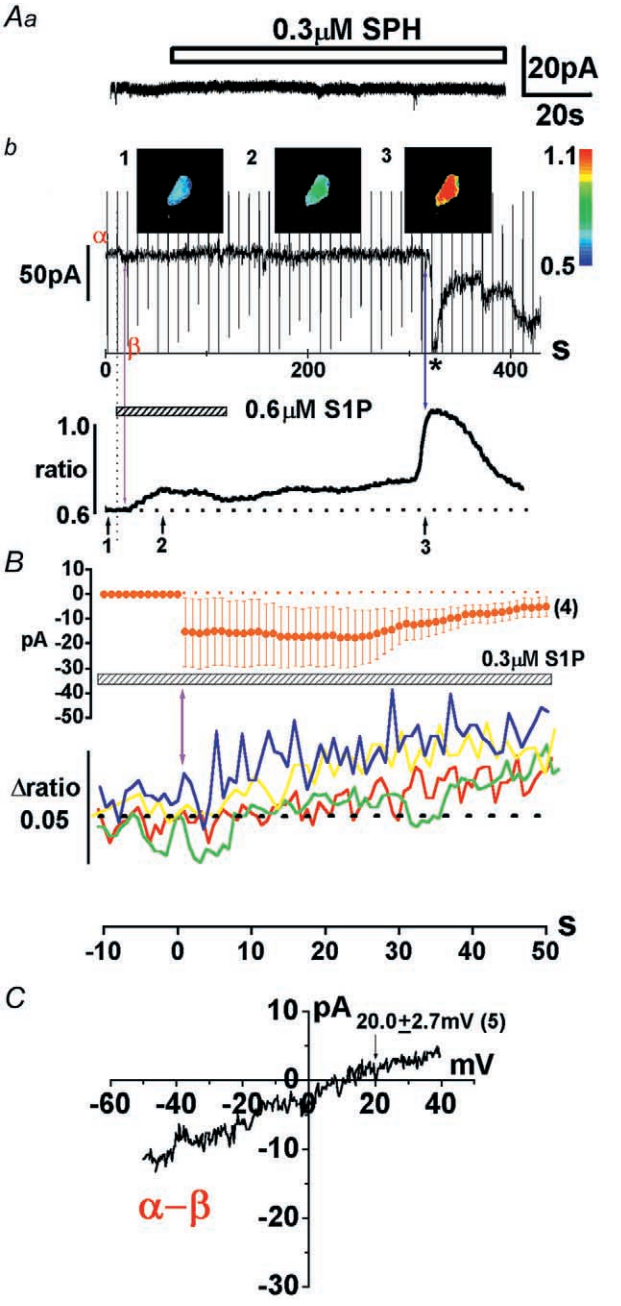

Figure 4. I_{NSC} activated by S1P in HUVECs

Aa, 0.3 μM SPH, a negative control lipid, had no effect on membrane currents at a holding potential of −50 mV. *Ab*, this cell was voltage clamped at −50 mV while $[Ca^{2+}]_i$ was monitored. The ramp waveform (0.96 V s^{-1}) was applied every 10 s. *Ab*, the change in the holding current and the corresponding fura-2 signal (F_{340}/F_{380} ratio) in the whole cell are plotted against time. The Ca^{2+} images indicated by 1–3 in the upper panel were taken at the times shown in the lower panel. Sampling frequency of Ca^{2+}-imaging apparatus was 1 Hz. The calibration of fluorescence ratio is indicated by the colour scale on the right. *B*, summary of the onset of the elevation of $[Ca^{2+}]_i$ and activation of I_{S1P}. The onset time of I_{S1P} was normalized to 0 s in four separate cells. The amplitude of I_{S1P} at −50 mV was averaged in the upper panel and the corresponding change of fluorescence ratio is plotted against time in the lower panel. *C*, the current–voltage (*I–V*) relationship of I_{NSC} activated by S1P under the physiological experimental conditions. This *I–V* relationship was obtained by subtracting the net membrane current in the presence of S1P (β in *Ab*) from that in its absence (α in *Ab*).

wortmannin for 60 min nor that with 20 μM PD98059 for 30 min altered the change in $[Ca^{2+}]_i$ of HUVECs following 0.3 μM S1P application (109.9 $\pm$ 13.5 nM, $n = 11$, 83.7 $\pm$ 7.6 nM, $n = 12$, respectively). These findings suggest that a PTX-sensitive G-protein mediates the change in $[Ca^{2+}]_i$ induced by S1P, and that neither PI3 kinase nor MAP kinase is involved.

Activation of non-selective cation currents by S1P in HUVECs

The preliminary data suggest that S1P can activate Ca^{2+} entry channels in HUVECs (see Fig. 2). Accordingly, we applied the amphotericin B-perforated-patch clamp technique in an effort to record S1P-induced membrane currents (Fig. 4). Cells were superfused with potassium aspartate-rich pipette solution. In some experiments, changes in membrane currents and $[Ca^{2+}]_i$ were simultaneously measured. As shown in Fig. 4*Aa*, 0.3 μM SPH (a negative control lipid) had no effect on membrane currents at a holding potential of -50 mV ($n = 4$). In contrast, application of 0.6 μM S1P consistently elicited a

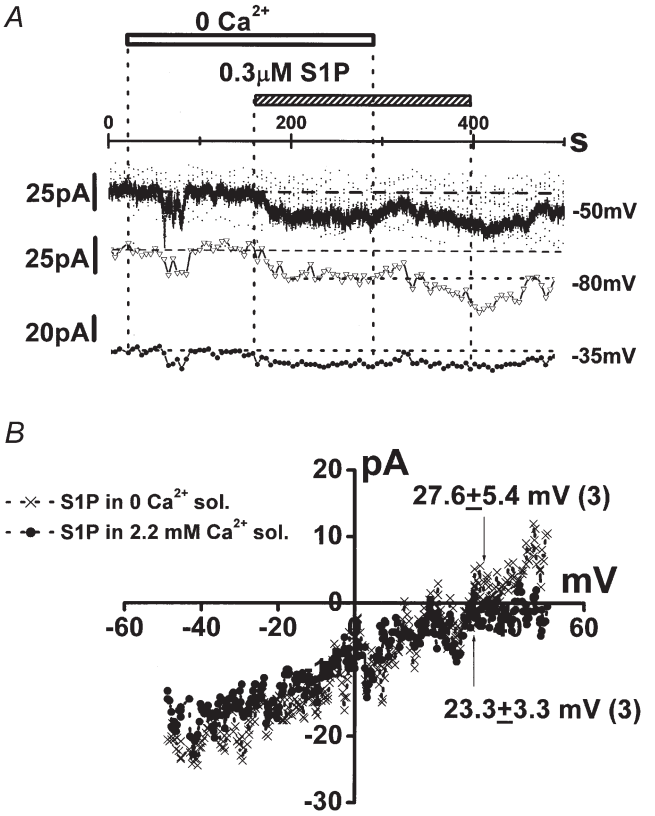

Figure 5. S1P-induced I_{NSC} in the absence and presence of external Ca^{2+}

A, the same experimental protocol as that in Fig. 2*B* was applied to a cell that was voltage clamped at -50 mV. The ramp waveform (0.96 V s^{-1}) was applied every 10 s. The scattered noisy spots shown in the original current trace were elicited by these ramp pulses. The original current trace and the change in the current amplitude at -80 and -35 mV, which were close to theoretical reversal potentials of K^+ and Cl^- currents, respectively, are shown. *B*, the *I–V* relationship of S1P-induced I_{NSC} with and without external Ca^{2+}. This difference was obtained by subtracting the net membrane current in the absence of Ca^{2+} from that in its presence. Arrows indicate the reversal potential of I_{NSC} with and without Ca^{2+}.

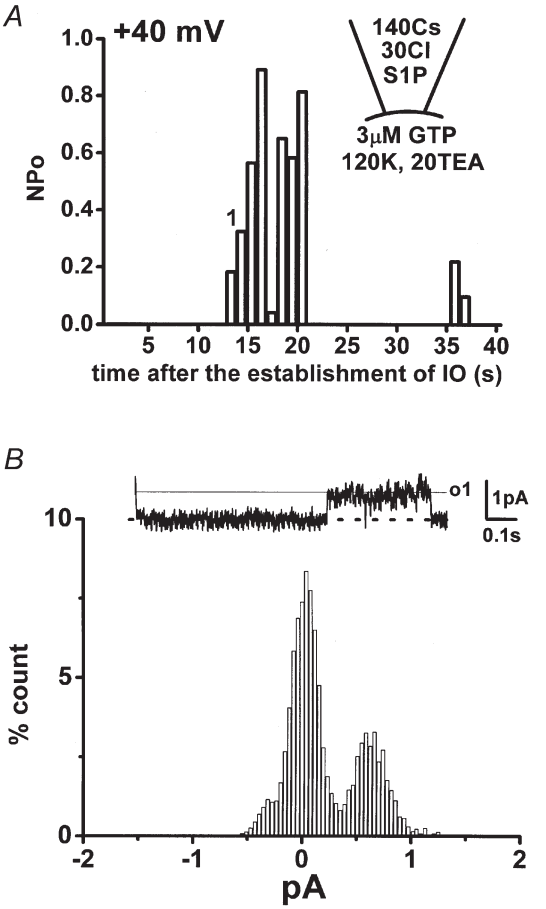

Figure 6. Single NSC channel current activated by S1P

NSC channels were activated by application of 0.3 μM S1P and 3 μM GTP in the inside-out patch configuration. The holding potential was +40 mV. *A*, changes in the relative open-state probability of channels (NP_o), which was calculated every 1024 ms, were plotted against time after the establishment of the excised inside-out (IO) configuration. *B*, the trace illustrated was obtained at the corresponding time indicated by '1' in *A* and the amplitude histogram was constructed. The *y*-axis (% count) expresses the relative time (%) at the corresponding amplitude in each bin *vs.* the total recording. The dashed line indicates the zero current level and o1 the open channel level for one channel. The single channel current amplitude and NP_o calculated from the histogram were 0.62 pA and 0.32, respectively. The bin width was 0.08 pA. The pipette and external solution mainly contained 110 mM caesium aspartate and 30 mM CsCl, and 120 mM KCl and 20 mM TEA-Cl, respectively.

small inward current (I_{S1P}). This was followed by an elevation of $[Ca^{2+}]_i$ after 1–4 s delay (purple arrow in Fig. 4*Ab*). Even after the removal of S1P, the elevation of $[Ca^{2+}]_i$ remained (as shown previously in Figs 1 and 2). Note also that the tiny I_{S1P} was maintained during the elevation of $[Ca^{2+}]_i$. The amplitude of I_{S1P} at −35 mV where the contamination with Cl^- currents was negligible was −19.4 ± 2.9 pA ($n = 5$). As indicated by the asterisk in Fig. 4*Ab*, a larger inward current was suddenly activated about 200 s after the washout of S1P. This was probably due to a direct membrane effect of S1P. However, this inward current followed the elevation of $[Ca^{2+}]_i$ (blue arrow in Fig. 4*Ab*). In Fig. 4*B*, the time course of the onset of the elevation of $[Ca^{2+}]_i$ is compared with that of the activation of I_{S1P}, demonstrating that I_{S1P} is activated prior to the elevation of $[Ca^{2+}]_i$. The onset time of I_{S1P} was normalized to zero in each cell ($n = 4$). The amplitude of I_{S1P} at −50 mV is averaged in the upper panel and the corresponding change of fluorescence ratio is plotted against time in the lower panel. The current–voltage relationship for I_{S1P} was determined using a ramp waveform applied immediately after the activation of I_{S1P} (β in Fig. 4*Ab*). As shown in Fig. 4*C*, I_{S1P} reversed at 20.0 ± 2.7 mV ($n = 5$) under these experimental conditions, suggesting that a previously identified type of NSC current (I_{NSC}) is responsible for I_{S1P} (Kamouchi *et al.* 1999*a*).

In Fig. 5, the same experimental protocol as that in Fig. 2*B* was utilized to record membrane currents at −50 mV. Ramp waveforms were applied every 10 s. The current amplitude at −80 and −35 mV where K^+ and Cl^- currents, respectively, theoretically closely reversed under these experimental conditions was also measured and plotted against time. Since the activation of K^+ currents was quite small, the change of amplitude of I_{S1P} at −80 and −35 mV denotes the change in both Cl^- currents and I_{NSC}, or only I_{NSC}, respectively. The application of 0.3 μM S1P in the absence of Ca^{2+} activated I_{S1P} at −35 and −80 mV, as well as at the holding potential of −50 mV. The addition of Ca^{2+} increased I_{S1P} at −80 mV (after 60–70 s delay), while at −35 mV there was no change in I_{S1P}. These findings suggest that I_{NSC} is activated independently of external Ca^{2+}. On the other hand, Cl^- currents were activated only in the presence of Ca^{2+}. Figure 5*B* shows that the reversal potential of I_{S1P} in the absence of Ca^{2+} was not significantly different from that in its presence (27.6 ± 5.4 and 23.3 ± 3.3 mV, respectively, $n = 3$). Since the pipette solution did not include Na^+, $[Na^+]_i$ was probably reduced to less than 0.3 mM after the establishment of the whole-cell configuration. According to eqns (1) and (2), these reversal potentials suggest that the permeability of K^+ relative to that of Na^+ is 1.02 (regardless of the $[Na^+]_i$ change from 0 to 0.3 mM), whereas that of Ca^{2+} is less than 0.06. In summary, these findings strongly suggest that S1P activates a I_{NSC} which may contribute to the elevation of $[Ca^{2+}]_i$ in HUVECs.

NSC channels activated by S1P in HUVECs

Figure 6 shows a single channel current record obtained in the excised inside-out patch configuration when the pipette and external solution contained 0.3 μM S1P and 3 μM GTP, respectively. To inhibit K^+ channel activity, the pipette and external solution contained 140 mM Cs^+

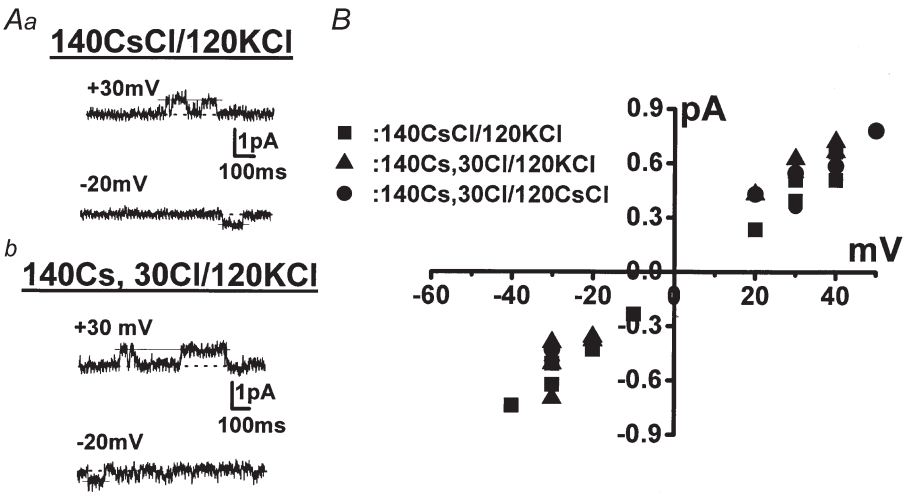

Figure 7. Current–voltage relationships of the NSC channel under various experimental conditions

A, original current traces obtained when the pipette solution contained mainly 140 mM CsCl (*a*) and 30 mM CsCl with 110 mM caesium aspartate (*b*), respectively. The bathing solution contained 120 mM KCl and 20 mM TEA-Cl. The dotted line indicates the zero current level. *B*, current amplitudes plotted against applied potentials. The channel activity was recorded in the inside-out patch configuration. The conductance and the reversal potential were estimated by fitting the set of data under each experimental condition to a regression line (see text).

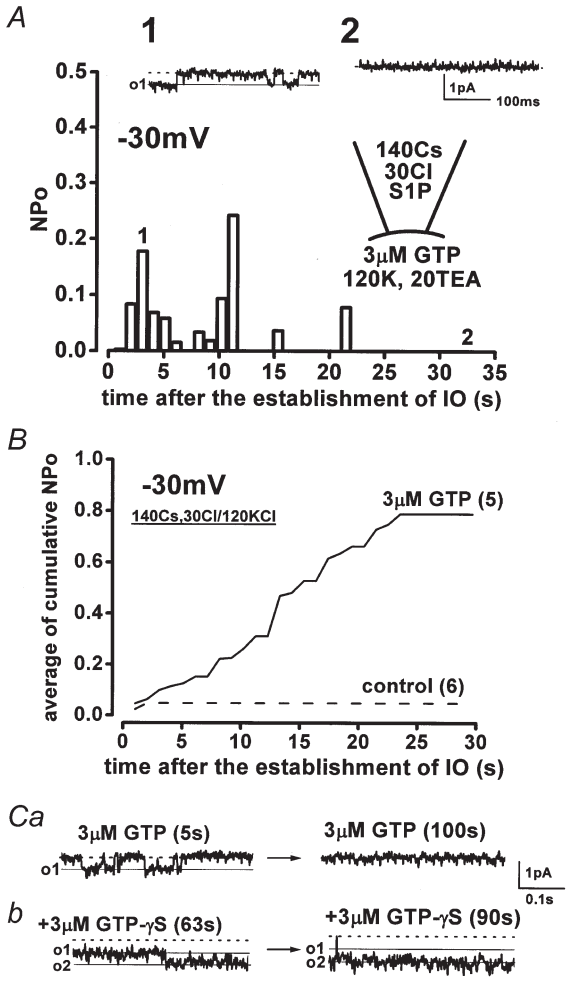

Figure 8. GTP-dependent activation of the NSC channel

A, in the lower panel, NP_o, which was calculated every 1024 ms, is plotted against time. The traces illustrated in the upper panel were obtained at the corresponding times indicated by '1' and '2' in the lower panel. S1P (0.3 μM) and GTP were present in the pipette and the bathing solution, respectively. *B*, summarized data describing the effect of intracellular GTP on the activity of NSC channels. The cumulative NP_o in the presence and absence (control) of 3 μM GTP in the bathing solution was pooled, and the mean values were plotted against time after the establishment of the excised inside-out patch configuration. The numbers in parentheses indicate the number of cells examined. *C*, recovery of the NSC channel activity from run-down by application of 3 μM GTP-γS. The values in parentheses show the elapsed time after exposure of the patch to GTP and GTP-γS. o1 and o2 indicate the opening level of one and two channels, respectively. Throughout these experiments, the patch membrane was held at −30 mV. The pipette and external solution mainly contained 110 mM caesium aspartate and 30 mM CsCl, and 120 mM KCl and 20 mM TEA-Cl, respectively.

and 20 mM TEA^+, respectively. To remove Cl^- channel currents, the 110 mM Cl^- in the pipette solution was replaced with equimolar $aspartate^-$, shifting the reversal potential of Cl^- to +34 mV. The Ca^{2+} concentration in the bathing solution was adjusted to pCa 7 with Ca^{2+}-EGTA buffer. Under these experimental conditions, a single channel current with a unitary current of 0.62 pA was recorded at a holding potential of +40 mV (Fig. 6*A* and *B*). The channel activity was detected in approximately 5% of membrane patches. When 0.3 μM S1P in the pipette solution was replaced with equimolar SPH, no channel activity was detected under the same experimental conditions ($n > 15$). The single channel conductance measured in the excised inside-out patch mode under superfusion with 120 mM K^+ in the bathing solution was 16.6 ± 1.5 pS ($n = 4$, Fig. 7*Ab* and *B*, triangles). The reversal potential of this single channel current was +2.3 ± 3.0 mV ($n = 4$), as predicted for a NSC channel (Kamouchi *et al.* 1999*a*). Substituting $aspartate^-$ in the pipette solution for Cl^- did not affect either the reversal potential (+5.3 mV, $n = 2$, Fig. 7*Aa* and *B*, squares), or the single channel conductance (16.9 pS, $n = 2$), excluding the possibility of Cl^- permeability. When K^+ in the bathing solution was replaced with Cs^+, the single channel conductance and the reversal potential were 16.5 ± 1.5 pS and +4.0 ± 4.0 mV ($n = 3$, Fig. 7*B*, circles), respectively. These results suggest that the 17 pS NSC is approximately equally permeable to K^+ and Cs^+.

The dependence on GTP of the activation of NSC channels was examined. Figure 8 shows inside-out patch recordings at −30 mV. When the pipette solution contained 110 mM caesium aspartate and 30 mM CsCl, the non-selective cation channels carried an inward Cs^+ current. This was the case in the presence of 3 μM GTP in the bathing solution as shown in Fig. 8*A*. The NSC channels were seldom active in the absence of GTP, and they showed significantly faster run-down in the absence of GTP (Fig. 8*B*). The activity of NSC channels disappeared within 120 s after the establishment of the inside-out patch configuration in the presence of GTP. The GTP dependence was therefore studied in detail. The relative open-state probability (NP_o) over 25 s after the establishment of the excised inside-out patch configuration in the presence of 3 μM GTP was significantly higher than that in its absence (0.034 ± 0.0094, $n = 5$, *vs.* 0.0021 ± 0.0011, $n = 6$, $P < 0.05$). The channel activity in the absence of GTP never recovered from run-down even with application of 3–10 μM GTP ($n = 5$). In contrast, after run-down, exposure of the patch membrane to 3 μM GTP-γS restored the channel activity (Fig. 8*Cb*, $n = 5$); on average it took 37.5 ± 11.8 s ($n = 5$) to reactivate the channel after treatment with GTP-γS. In the presence of GTP-γS, channel opening was noisy. The NP_o (which appeared to be more than 1.0), could not be therefore determined (right panel in Fig. 8*Cb*).

DISCUSSION

These results demonstrate that S1P increases $[Ca^{2+}]_i$ in HUVECs via Ca^{2+} entry and that this effect involves the activation of a PTX-sensitive G-protein. Moreover, here we show for the first time a function of S1P to activate NSC channels with a conductance of 17 pS in a GTP-dependent manner. The NSC channels may play an obligatory role in S1P-mediated Ca^{2+} entry in human endothelial cells.

Ca^{2+} response of HUVECs to S1P and SPH

Our findings that the EC_{50} of S1P for elevation of $[Ca^{2+}]_i$ in HUVECs was 63 nM and that concentrations of SPH less than 1 μM had no effect on $[Ca^{2+}]_i$ suggest that S1P elevates $[Ca^{2+}]_i$ via stimulation of edgs without direct membrane effects. Consistently, S1P was found to bind effectively to edg-1, whereas SPH did not (Lee *et al.* 1998). It has been shown that S1P is present in human plasma and serum at a concentration of 200 and 500 nM, respectively, and thus human endothelial cells are constantly exposed to S1P (Yatomi *et al.* 1997). However, it has not been clear whether under these physiological conditions, edgs are activated, and consequently transduce biological signals without desensitization. S1P and sphingosylphosphocholine, which is also present in mammalian plasma/serum and stimulates edgs, affected membrane currents in freshly isolated cardiac myocytes, whereas it is not clear whether S1P affects $[Ca^{2+}]_i$ in endothelial cells *in situ* (Bunemann *et al.* 1995; Guo *et al.* 1999; Himmel *et al.* 2000; Liliom *et al.* 2001). In our preliminary experiments, application of 0.3 μM S1P to rabbit aorta with intact endothelium caused an endothelium-dependent relaxation (K. Muraki & Y. Imaizumi, unpublished observations). Thus, it is possible that edgs in endothelium are not desensitized even by exposure to plasma and serum.

Signal transduction mechanisms involved in the elevation of $[Ca^{2+}]_i$ by S1P and histamine

The major finding presented here is that in HUVECs, S1P predominantly utilizes Ca^{2+} from the extracellular space. Despite extensive studies, the mechanism involved in the mobilization of Ca^{2+} via stimulation of edg-1 has not been determined (Pyne & Pyne, 2000). Since the S1P-induced Ca^{2+} response occurred without the production of $InsP_3$ and was resistant to removal of external Ca^{2+} (Mattie *et al.* 1994), it was proposed that S1P directly releases Ca^{2+} from Ca^{2+} stores as an intracellular second messenger. In our experiments, 90% of HUVECs exhibited no S1P-induced change in $[Ca^{2+}]_i$ in the absence of external Ca^{2+}, and SK&F96365 significantly inhibited the S1P-induced elevation of $[Ca^{2+}]_i$ (Fig. 2). Moreover, I_{NSC}, which allows Ca^{2+} to enter cells, was activated before the elevation of $[Ca^{2+}]_i$ occurred (Fig. 4). An obligatory event in the pathway involved in S1P-induced elevation of $[Ca^{2+}]_i$ in HUVECs is the activation of I_{NSC} (see below).

In approximately 10% of HUVECs, S1P slightly but significantly increased $[Ca^{2+}]_i$ even in the absence of external Ca^{2+}. Since we did not use any Ca^{2+} chelators to remove Ca^{2+} (nominally Ca^{2+} free), these HUVECs might have responses to S1P using the residual Ca^{2+} in the bathing solution. Alternatively, and more likely, other edgs may be expressed in HUVECs; if so, they could mediate Ca^{2+} responses via release of Ca^{2+} from Ca^{2+} stores. Northern blot analysis has revealed that HUVECs have *edg-3* as well as *edg-1*, and that the expression level of *edg-3* is much lower than that of *edg-1* (Lee *et al.* 1999). Edg-3 couples to Gq-protein, resulting in the production of $InsP_3$, which releases Ca^{2+} from intracellular Ca^{2+} stores (Yamaguchi *et al.* 1996; Ancellin & Hla, 1999). However, we cannot completely rule out the possibility that S1P is an intracellular second messenger. It has been suggested that the edg-1-mediated Ca^{2+} response is cell-type specific (Zondag *et al.* 1998). Moreover, the present results provide the evidence that neither MAP nor PI3 kinase is involved in the S1P-induced elevation of $[Ca^{2+}]_i$ in HUVECs.

The elevation of $[Ca^{2+}]_i$ by histamine in HUVECs was much less sensitive to PTX, but, nevertheless, significantly inhibited by PTX. The histamine receptor subtype expressed in HUVECs is mainly histamine H1 receptor: it is widely distributed in peripheral tissues and the central nervous system, and is primarily coupled to the activation of PLC via a PTX-insensitive G-protein (Hill *et al.* 1997). It is, however, possible that in HUVECs histamine receptors are in part coupled to a PTX-sensitive G-protein. Consistently, half of the response of rabbit aortic endothelial cells to acetylcholine (ACh) (which is mediated by the same type of G-proteins to histamine) is inhibited by the PTX treatment (Taki *et al.* 1999). Nevertheless, we cannot rule out the possibility that PTX inhibits cellular responses non-specifically.

Activation of NSC channels by S1P in HUVECs

In the present study, we have provided novel, direct evidence that S1P can activate I_{NSC}, and that in HUVECs the underlying unitary conductance is a 17 pS channel. Although the delayed activation of Cl^- current by S1P in the presence of Ca^{2+} complicates the interpretation of our results (Fig. 5*A*), this I_{NSC} is permeable to Na^+, Cs^+ and K^+ ($P_K/P_{Na} = 1.02$) but not to Cl^-. The reversal potential for I_{NSC} is close to the theoretical equilibrium potential of cations (+10 to +20 mV) and the substitution of aspartate$^-$ for Cl^- did not change the reversal potential of the 17 pS NSC channel. Moreover, the I_{NSC} represents a significant entry pathway for Ca^{2+} in HUVECs in the presence of S1P. If intracellular Na^+ was assumed to be 0.1–0.3 mM, under the present experimental conditions, the permeability of Ca^{2+} was estimated to be 1.8–6.4% of that of Na^+. Thus, although the I_{NSC} has a low permeability to Ca^{2+}, nevertheless, Ca^{2+} does enter the cell. In immortalized human endothelial cells (Ea.hy 926

cells), ATP activates a I_{NSC} generated by a channel with a conductance of 24 pS (Kamouchi *et al.* 1999*a*). The permeability of the I_{NSC} in Ea.hy 926 cells to Ca^{2+} is quite low compared to that of Na^+ (~7 %). Despite this similarity in characteristics between ATP-induced I_{NSC}/24 pS NSC channels in Ea.hy926 cells and S1P-induced I_{NSC}/17 pS NSC channels, these entities are clearly distinct. For example: (i) elevation of $[Ca^{2+}]_i$ follows S1P-induced I_{NSC} (Fig. 4*A* and *B*); (ii) a PTX-sensitive G-protein is predominantly involved in the signal transduction leading to the elevation of $[Ca^{2+}]_i$ by S1P (Fig. 3); (iii) the amplitude of I_{NSC} in the absence of external Ca^{2+} is similar to that in its presence (Fig. 5). None of these were observed in Ea.hy 926 cells.

In vascular endothelial cells, several types of transient receptor potential (Trp channel), which resemble certain types of cation channel, are expressed (Chang *et al.* 1997; Nilius *et al.* 1997; Groschner *et al.* 1998; Kamouchi *et al.* 1999*b*). It is not clear whether the 17 pS NSC channel in the present study is a member of the Trp channel family because characteristics of all Trp channels have not been fully investigated (Harteneck *et al.* 2000). However, since S1P-induced elevation of $[Ca^{2+}]_i$ in HUVECs was inhibited by SK&F96365, a Trp channel is a possible candidate for the S1P-induced NSC channel. Both Trp6 and Trp7 channels are inhibited by SK&F96365 (Okada *et al.* 1999; Inoue *et al.* 2001). Quite recently, an elegant new method for peptide-specific binding of the antibody to TrpC1 (a store-operated Ca^{2+} channel activity in native smooth muscle cells) has been introduced (Xu & Beech, 2001). In principal, this approach will be useful to identify the Trp channel that is responsible for I_{NSC} in HUVECs.

Using inside-out patch recording, we have directly demonstrated that the presence of GTP in the bathing solution allowed S1P-induced NSC channels to maintain their activity. Moreover, after run-down, the activity of NSC channels was recovered by application of GTP-γS, indicating that the channel activity is regulated by a GTP-dependent process, e.g. interaction with G-proteins. When cardiac myocytes were exposed to S1P, ACh-activated K^+ channels (GIRK channels) were activated (Bunemann *et al.* 1995; Guo *et al.* 1999; Himmel *et al.* 2000). The activity of GIRK channels, which are one of the effectors for S1P in cardiac myocytes, is also regulated by intracellular GTP and GTP-γS (Kurachi *et al.* 1986; Kurachi, 1995). In ilial smooth muscles, ACh-induced NSC channels are sensitive to PTX treatment and activated by GTP-γS infusion (Inoue & Isenberg, 1990). However, since it has been reported that many factors such as Ca^{2+}, lipids and kinases as well as G-proteins regulate the activity of NSC channels in various types of cell (Barritt, 1999), we cannot rule out the possibility that such mechanisms are affected by GTP-dependent processes and involved in the regulation of S1P-induced NSC channels in HUVECs.

An, S., Bleu, T., Hallmark, O. G. & Goetzl, E. J. (1998). Characterization of a novel subtype of human G protein-coupled receptor for lysophosphatidic acid. *Journal of Biological Chemistry* **273**, 7906–7910.

Ancellin, N. & Hla, T. (1999). Differential pharmacological properties and signal transduction of the sphingosine 1-phosphate receptors EDG-1, EDG-3, and EDG-5. *Journal of Biological Chemistry* **274**, 18997–19002.

Barritt, G. J. (1999). Receptor-activated Ca^{2+} inflow in animal cells: a variety of pathways tailored to meet different intracellular Ca^{2+} signalling requirements. *Biochemical Journal* **337**, 153–169.

Bunemann, M., Brandts, B., zu Heringdorf, D. M., van Koppen, C. J., Jakobs, K. H. & Pott, L. (1995). Activation of muscarinic K^+ current in guinea-pig atrial myocytes by sphingosine-1-phosphate. *Journal of Physiology* **489**, 701–777.

Chang, A. S., Chang, S. M., Garcia, R. L. & Schilling, W. P. (1997). Concomitant and hormonally regulated expression of trp genes in bovine aortic endothelial cells. *FEBS Letters* **415**, 335–340.

Groschner, K., Hingel, S., Lintschinger, B., Balzer, M., Romanin, C., Zhu, X. & Schreibmayer, W. (1998). Trp proteins form store-operated cation channels in human vascular endothelial cells. *FEBS Letters* **437**, 101–106.

Guo, J., MacDonell, K. L. & Giles, W. R. (1999). Effects of sphingosine 1-phosphate on pacemaker activity in rabbit sino-atrial node cells. *Pflügers Archiv* **438**, 642–648.

Harteneck, C., Plant, T. D. & Schultz, G. (2000). From worm to man: three subfamilies of TRP channels. *Trends in Neurosciences* **23**, 159–166.

Hecht, J. H., Weiner, J. A., Post, S. R. & Chun, J. (1996). Ventricular zone gene-1 (vzg-1) encodes a lysophosphatidic acid receptor expressed in neurogenic regions of the developing cerebral cortex. *Journal of Biological Chemistry* **135**, 1071–1083.

Hill, S. J., Ganellin, C. R., Timmerman, H., Schwartz, J. C., Shankley, N. P., Young, J. M., Schunack, W., Levi, R. & Haas, H. L. (1997). International Union of Pharmacology. XIII. Classification of histamine receptors. *Pharmacological Review* **49**, 253–278.

Himmel, H. M., Meyer Zu, H. D., Graf, E., Dobrev, D., Kortner, A., Schuler, S., Jakobs, K. H. & Ravens, U. (2000). Evidence for Edg-3 receptor-mediated activation of $I_{K.ACh}$ by sphingosine-1-phosphate in human atrial cardiomyocytes. *Molecular Pharmacology* **58**, 449–454.

Hla, T., Lee, M. J., Ancellin, N., Liu, C. H., Thangada, S., Thompson, B. D. & Kluk, M. (1999). Sphingosine-1-phosphate: extracellular mediator or intracellular second messenger? *Biochemical Pharmacology* **58**, 201–207.

Hla, T. & Maciag, T. (1990). An abundant transcript induced in differentiating human endothelial cells encodes a polypeptide with structural similarities to G-protein-coupled receptors. *Journal of Biological Chemistry* **265**, 9308–9313.

Igarashi, J., Bernier, S. G. & Michel, T. (2001). Sphingosine 1-phosphate and activation of endothelial nitric-oxide synthase. differential regulation of Akt and MAP kinase pathways by EDG and bradykinin receptors in vascular endothelial cells. *Journal of Biological Chemistry* **276**, 12420–12426.

Imaizumi, Y., Muraki, K. & Watanabe, M. (1989). Ionic currents in single smooth muscle cells from the ureter of the guinea-pig. *Journal of Physiology* **411**, 131–159.

Inoue, R. & Isenberg, G. (1990). Acetylcholine activates nonselective cation channels in guinea pig ileum through a G protein. *American Journal of Physiology* **258**, C1173–1178.

Inoue, R., Okada, T., Onoue, H., Hara, Y., Shimizu, S., Naitoh, S., Ito, Y. & Mori, Y. (2001). The transient receptor potential protein homologue TRP6 is the essential component of vascular α_1-adrenoceptor-activated Ca^{2+}-permeable cation channel. *Circulation Research* **88**, 325–332.

Kamouchi, M., Mamin, A., Droogmans, G. & Nilius, B. (1999*a*). Nonselective cation channels in endothelial cells derived from human umbilical vein. *Journal of Membrane Biology* **169**, 29–38.

Kamouchi, M., Philipp, S., Flockerzi, V., Wissenbach, U., Mamin, A., Raeymaekers, L., Eggermont, J., Droogmans, G. & Nilius, B. (1999*b*). Properties of heterologously expressed hTRP3 channels in bovine pulmonary artery endothelial cells. *Journal of Physiology* **518**, 345–358.

Kurachi, Y. (1995). G protein regulation of cardiac muscarinic potassium channel. *American Journal of Physiology* **269**, C821–830.

Kurachi, Y., Nakajima, T. & Sugimoto, T. (1986). Acetylcholine activation of K^+ channels in cell-free membrane of atrial cells. *American Journal of Physiology* **251**, H681–684.

Lee, H., Goetzl, E. J. & An, S. (2000). Lysophosphatidic acid and sphingosine 1-phosphate stimulate endothelial cell wound healing. *American Journal of Physiology* **278**, C612–618.

Lee, M. J., Thangada, S., Claffey, K. P., Ancellin, N., Liu, C. H., Kluk, M., Volpi, M., Sha'afi, R. I. & Hla, T. (1999). Vascular endothelial cell adherens junction assembly and morphogenesis induced by sphingosine-1-phosphate. *Cell* **99**, 301–312.

Lee, M. J., Van Brocklyn, J. R., Thangada, S., Liu, C. H., Hand, A. R., Menzeleev, R., Spiegel, S. & Hla, T. (1998). Sphingosine-1-phosphate as a ligand for the G protein-coupled receptor EDG-1. *Science* **279**, 1552–1555.

Liliom, K., Sun, G., Bunemann, M., Virag, T., Nusser, N., Baker, D. L., Wang, D. A., Fabian, M. J., Brandts, B., Bender, K., Eickel, A., Malik, K. U., Miller, D. D., Desiderio, D. M., Tigyi, G. & Pott, L. (2001). Sphingosylphosphocholine is a naturally occurring lipid mediator in blood plasma: a possible role in regulating cardiac function via sphingolipid receptors. *Biochemical Journal* **355**, 189–197.

Liu, Y., Wada, R., Yamashita, T., Mi, Y., Deng, C. X., Hobson, J. P., Rosenfeldt, H. M., Nava, V. E., Chae, S. S., Lee, M. J., Liu, C. H., Hla, T., Spiegel, S. & Proia, R. L. (2000). Edg-1, the G protein-coupled receptor for sphingosine-1-phosphate, is essential for vascular maturation. *Journal of Clinical Investigation* **106**, 951–961.

Mattie, M., Brooker, G. & Spiegel, S. (1994). Sphingosine-1-phosphate, a putative second messenger, mobilizes calcium from internal stores via an inositol trisphosphate-independent pathway. *Journal of Biological Chemistry* **269**, 3181–3188.

Muraki, K. & Imaizumi, Y. (2001). On the mechanism of activation of a non-selective cation channel by sphingosine-1-phosphate in human endothelial cells. *Japanese Journal of Pharmacology* **85**, 67P.

Muraki, K., Imaizumi, Y., Ohya, S., Sato, K., Takii, T., Onozaki, K. & Watanabe, M. (1997). Apamin-sensitive Ca^{2+}-dependent K^+ current and hyperpolarization in human endothelial cells. *Biochemical and Biophysical Research Communications* **236**, 340–343.

Nilius, B., Viana, F. & Droogmans, G. (1997). Ion channels in vascular endothelium. *Annual Review of Physiology* **59**, 145–170.

Okada, T., Inoue, R., Yamazaki, K., Maeda, A., Kurosaki, T., Yamakuni, T., Tanaka, I., Shimizu, S., Ikenaka, K., Imoto, K. & Mori, Y. (1999). Molecular and functional characterization of a novel mouse transient receptor potential protein homologue TRP7. Ca^{2+}-permeable cation channel that is constitutively activated and enhanced by stimulation of G protein-coupled receptor. *Journal of Biological Chemistry* **274**, 27359–27370.

Okazaki, H., Ishizaka, N., Sakurai, T., Kurokawa, K., Goto, K., Kumada, M. & Takuwa, Y. (1993). Molecular cloning of a novel putative G protein-coupled receptor expressed in the cardiovascular system. *Biochemical and Biophysical Research Communications* **190**, 1104–1109.

Pyne, S. & Pyne, N. J. (2000). Sphingosine 1-phosphate signalling in mammalian cells. *Biochemical Journal* **349**, 385–402.

Taki, H., Muraki, K., Imaizumi, Y. & Watanabe, M. (1999). Mechanisms of the palmitoylcarnitine-induced response in vascular endothelial cells. *Pflügers Archiv* **438**, 463–469.

Van Brocklyn, J. R., Lee, M. J., Menzeleev, R., Olivera, A., Edsall, L., Cuvillier, O., Thomas, D. M., Coopman, P. J., Thangada, S., Liu, C. H., Hla, T. & Spiegel, S. (1998). Dual actions of sphingosine-1-phosphate: extracellular through the G_i-coupled receptor Edg-1 and intracellular to regulate proliferation and survival. *Journal of Cell Biology* **142**, 229–240.

Vennekens, R., Hoenderop, J. G., Prenen, J., Stuiver, M., Willems, P. H., Droogmans, G., Nilius, B. & Bindels, R. J. (2000). Permeation and gating properties of the novel epithelial Ca^{2+} channel. *Journal of Biological Chemistry* **275**, 3963–3969.

Wang, F., Van Brocklyn, J. R., Hobson, J. P., Movafagh, S., Zukowska-Grojec, Z., Milstien, S. & Spiegel, S. (1999). Sphingosine 1-phosphate stimulates cell migration through a G_i-coupled cell surface receptor. Potential involvement in angiogenesis. *Journal of Biological Chemistry* **274**, 35343–35350.

Xu, S. Z. & Beech, D. J. (2001). TrpC1 is a membrane-spanning subunit of store-operated Ca^{2+} channels in native vascular smooth muscle cells. *Circulation Research* **88**, 84–87.

Yamaguchi, F., Tokuda, M., Hatase, O. & Brenner, S. (1996). Molecular cloning of the novel human G protein-coupled receptor (GPCR) gene mapped on chromosome 9. *Biochemical and Biophysical Research Communications* **227**, 608–614.

Yatomi, Y., Igarashi, Y., Yang, L., Hisano, N., Qi, R., Asazuma, N., Satoh, K., Ozaki, Y. & Kume, S. (1997). Sphingosine 1-phosphate, a bioactive sphingolipid abundantly stored in platelets, is a normal constituent of human plasma and serum. *Journal of Biochemistry* **121**, 969–973.

Zondag, G. C., Postma, F. R., Etten, I. V., Verlaan, I. & Moolenaar, W. H. (1998). Sphingosine 1-phosphate signalling through the G-protein-coupled receptor Edg-1. *Biochemical Journal* **330**, 605–609.

Acknowledgements

This work was supported by a grant from the Uehara Memorial Foundation and Grant-in-Aid for Scientific Research (C) from Japan Society for the Promotion of Science to K.M., and a Research Grant for Cardiovascular Diseases (12C-1) from the Ministry of Health and Welfare to Y.I. We thank Dr Asamoto for his help with our experiments. We also thank Dr W. Giles for supplying data-acquisition/analysis software and for critical reading of this manuscript. We are also grateful to Dr J. Dempster for supplying the data-analysis software.

Corresponding author

K. Muraki: Department of Molecular and Cellular Pharmacology, Graduate School of Pharmaceutical Sciences, Nagoya City University, 3-1 Tanabedori, Mizuhoku, Nagoya 467-8603, Japan.

Email: kmuraki@phar.nagoya-cu.ac.jp